Evaluation of flow resistance in unsteady pipe flow: numerical developments and first experimental results

Pedro Leite, Dídia I. C. Covas, Helena M. Ramos
Instituto Superior Técnico/Universidade Técnica de Lisboa

José Tentúgal Valente, Manuel Maria Pacheco Figueiredo
Faculdade de Engenharia da Universidade do Porto

ABSTRACT

The current paper presents the first results obtained in the investigation of flow resistance in pressurized pipes both through numerical developments and experimental analysis. 1D and quasi-2D mathematical models have been implemented by using the Method of Characteristics: the first is a classic transient solver and the latter follows Vardy and Hwang (1992)'s approach for the velocity profiles calculation in each pipe cross section.

A new experimental facility has been assembled at the Hydraulics Laboratory of Instituto Superior Técnico (IST/UTL), Lisbon, funded by the Portuguese Foundation for Science and Technology (FCT) through the project PTDC/ECM/112868/2009. The facility is composed of a pump with a nominal flow of 20 l/s and elevation of 38 m, a 1 m^3 hydropneumatic vessel and a steel pipe, 115 m long and with 200 mm diameter. The facility is equipped with instrumentation for collecting steady flow data (electromagnetic flow meter) and transient pressure data (pressure transducers).

First experimental data are presented and the main problems faced with data collection are discussed. Numerical results obtained by using the two transient solvers are compared. The first conclusions are drawn concerning experimental and numerical and the following steps of the project are presented.

Keywords: experimental facility; pipe flows, water hammer; transients; two-dimensional models;

NOTATION

The following symbols are used in this paper:

c = elastic wave speed (m.s^{-1});
g = gravity acceleration (m.s^{-2});
D = pipe inner diameter (m);
f = Darcy-Weisbach steady state friction factor (-);
H = piezometric head (m);
Re = Reynolds number (-);
t = time (s);
t_i = time corresponding to the beginning of the valve closure (s);
V = velocity (m.s^{-1});
x = coordinate along the pipe axis (m);
u_j = local axial velocity with index j (m.s^{-1});
v_j = lateral velocity component (m.s^{-1});
ρ = density (kg.m^{-3});
P_j = surface area at cylinder j (m^2);
Δt , Δx = time step (s) and space step (m);
ϵ = eddy viscosity (m^{2}s^{-1});
μ = dynamic viscosity (kg.m^{-1}s^{-1});
ν = kinematic viscosity (m^{2}s^{-1});
θ = weighting coefficients (-);
τ_j = shear stress of the fluid at the position with index j and j-1 (N.m^{-2}).

1   INTRODUCTION

Water pipeline systems are vital infrastructures that provide an indispensable public service to the society: the provision of safe drinking water and sanitation. These services are crucial to ensure the health and wellbeing of the populations. However, these systems are subjected to pressure surges as a result of pumps' start-up and trip-off or maneuvers in mechanical devices. The prediction of pressure surges is important in the design of pumped systems for the selection of pipe materials, pressure classes and surge protection devices. When severe transients cannot be avoided, either pipe layout or parameters are changed (*e.g*., operating conditions) or surge protection devices are specified (*e.g*., pressurized vessels or air-relief valves), so as to sustain maximum and minimum pressures within acceptable limits. Usually, the decision is the most economical and reliable solution that yields an acceptable transient pressure response. Hydraulic transient analysis is equally important for the diagnosis of existing operational problems (*e.g*., pipe failures, devices malfunctioning).

Extreme transient pressures calculated by most solvers are not accurate enough to describe the physical behavior observed in real life systems. One of the most common uncertainties is the calculation of pressure peaks and of energy dissipation due to the unsteady shear stress. As a result, transient pressure signal amplitude (initial peaks), phase and shape are often not well described, pipe systems are not well designed, resonance effects may take place and accidents can occur (*e.g*., the disaster in the Russia's largest hydro-electric power station in 17th August 2009); additionally, the diagnosis is not well supported, and causes of accidents are often not identified.

Unsteady-friction losses have been widely studied for the last fifty years. These losses are particularly relevant in fast transient events or high-oscillating frequencies. While an analytical solution has been derived for unsteady friction calculation in transient laminar flows (Zielke 1968; Trikha 1975), no universal formula exists yet for turbulent flows, though several approximate formulations have been presented based on: (i) instantaneous mean velocity (Hino et al. 1977); (ii) instantaneous acceleration (Shuy 1996); (iii) weights of past time local accelerations (Vardy et al. 1993); (iv) local and convective accelerations (Brunone et al.1995; Ramos et al. 2004; Vitkovsky et al. 2000); and (v) velocity profiles (Eichinger and Lein 1992; Silva-Araya and Chaudhry 1997; Pezzinga 1999; Vardy and Hwang 1991).

The current paper aims at the presentation of the first results of the experimental and numerical research of energy dissipation in transient flows due to unsteady skin friction carried out at Instituto Superior Tecnico, funded by the Portuguese Foundation for Science and Technology (FCT) through the project PTDC/ECM/112868/2009. A new experimental facility assembled at the Hydraulics Laboratory of Instituto Superior Técnico is described. First collected data are presented. A quasi-2D hydraulic transient solver was implemented and numerical results obtained are compared with classic 1D modelling. The next steps of the project are presented.

2 DATA COLLECTION AND ANALYSIS

2.1 Experimental facility description

Transient data were collected from tests carried out in a new experimental reversible pumping system assembled at the Hydraulics Laboratory of Instituto Superior Técnico (IST), Lisbon/Portugal, funded by the Portuguese Foundation for Science and Technology (FCT) through the project PTDC/ECM/112868/2009.

The facility is composed of pipeline made of steel, with a nominal pressure of 10 bar, a total length of 115 m and diameter of 200 mm. The pipeline is installed along the internal perimeter of the Laboratory (Figure 1). The system is supplied from a storage tank through a centrifugal pump with a nominal flow rate of 20 l/s, a nominal elevation of 38 m and a installed power of 15 kW, with a swing check-valve located at immediately downstream. A 1 m^3 hydro-pneumatic vessel is installed at downstream the pump; this device can be connected in-line, as a side element connected through a branch or totally disconnected from the system by the opening/closing of a set of gate valves (Figure 2). The flow can circulate in the pipeline in two directions, reason why it is called a reversible system. At the downstream end there are two ball valves with 50 mm diameter each, used to generate water hammer. There are several side discharge valves with ½" and ¾" for connecting pressure transducers and draining the accumulated air, respectively, and three 1" scour valves for draining the pipeline.

Currently, the facility is equipped with instrumentation for collecting steady flow data (electromagnetic flow meter ABB Processmaster FEP311-065 with 65 mm and accuracy of 0.4% of measured values) and transient pressure data (WIKA pressure transducers with an absolute pressure range from 0 to 25 bar and accuracy of 0.5% of full range); in the near future, sensors for collecting transient strain data (strain gauges), hot-films for collecting wall-shear stress and a particle image velocimetry (PIV) for measuring transient velocity profiles will be installed. A transparent box with a metal frame and with a cylindrical glass pipe inside will be installed at three different sections for measuring the velocity fields.
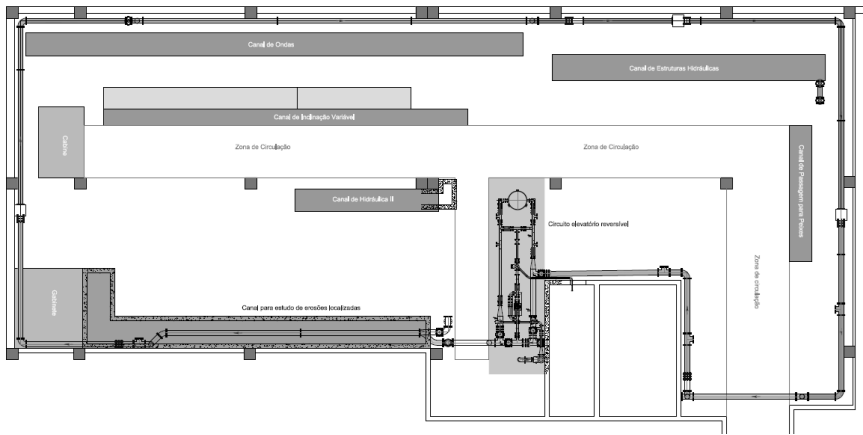
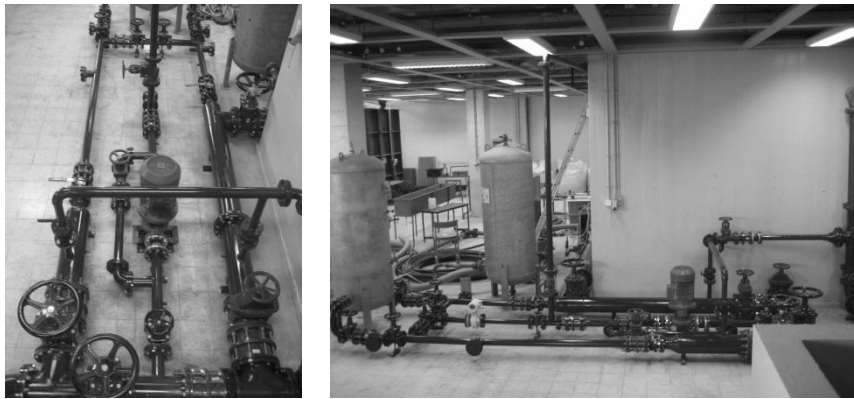**Figure 1 –Experimental reversible pumping system**

Figure 2 – Views of the pumping station.

2.2   Data Analysis

The first collected transient data are presented herein. Pressure was collected with a frequency of 500 hz at three different locations - T1, T2 and T3 - located, respectively, at upstream and downstream of the pump, and at the downstream the pipeline immediately upstream the ball valve. Transient tests were run for several consecutive days, for different initial flows, Q, between 2 and 18 L/s, with Reynolds numbers between 9700 and 87500. Two main problems have occurred.

The first problem was a high amplitude electric noise that was collected in the pressure signal. This noise is visible in Figure 3a, it has 20 m amplitude in steady state conditions and it is created by the pump and its frequency converter that allows the steady start-up and shut-down of the pump, as well as its operation different rotational speeds. It is transmitted through the electric network as well as radiated through the air as an electromagnetic field. This problem could be mitigated by: (i) filtering the pressure signal which has been done (see Figures 3b and 4a) which filters as well frequencies associated pipe feature reflections during transient tests; (ii) installing an electric filter at the velocity converted; (iii) using blinded cables with twisted wirepairs; (iv) changing the

data acquisition system (i.e., oscilloscope and pressure sensors) and instead of measuring the signal in terms of the electric potential difference (in volts) measuring in electric current (in ampere). Measure (i) was tested whose results are presented in Figure 3b. Later (in May 2012), measures (ii) and (iii) were implemented and the electric noise was significantly reduced as presented in Figure 4b.
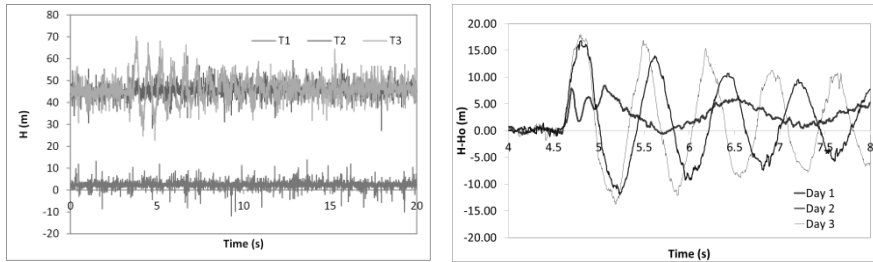

(a) Pressure signal at three locations for Q=5 l/s - Day 3 (March 2012)

(b) Filtered pressure signal at the downstream end of the pipeline (T3) in consecutive days for Q=5 l/s (March 2012)

Figure 3 – Collected transient pressure data

The second problem that occurred was the presence of air in the system. Gas can appear in pressurized pipes in three forms. Gas can be dissolved in the liquid; usually it is dissolved in very small quantities as there is a maximum concentration of dissolved gases which is a function of pressure and temperature; the liquid is described as monophasic. Second, gas can be in the liquid in a free form. Finally, gas can be cumulated in air pockets located at highest pipe sections or along quasi-horizontal pipes. In the current tests, air appeared in these three forms. Figure 3b shows the pressure signal collected in three consecutive days for the same flow rate (5 L/s): in Day 1 there were major air pockets in the pipeline that disappeared slowly along time, but it Day 3 there was still air in the liquid as the experimental wave speed (calculated based on the travelling time between transducers) was still much lower (900 m/s) than the theoretical value for a steel pipe with 200 mm diameter and a wall thickness of 15 mm (1300 m/s). Figure 4 shows several transient tests carried out in Day 3 for different flow rates. In order to eliminate the air pockets, eleven air valves were installed along the pipe and the cumulated air was significantly reduced (Figure 4b): measured wave speed increased from 900 to 1050 m/s.
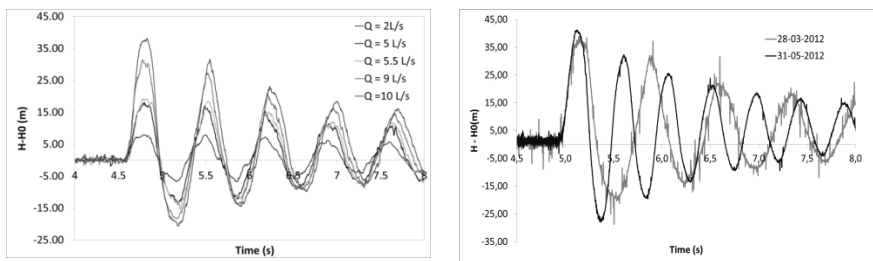
(a) Filtered pressure signal for different flow in Day 3 for different flow rates (March 2012)

(b) Comparison of the (unfiltered) pressure signal after obtained initially and 2 months after for Q=10 l/s

Figure 4 – Transient pressure signal at the downstream end of the pipeline (transducer T3)

3 QUASI-TWO-DIMENSIONAL MODEL

3.1 Introduction

Usually, one-dimensional (1-D) models are used to simulate hydraulic transients in pipe systems, as the pipe flow is mainly one-dimensional and these models are reasonably accurate and easy to implement in multi-pipe systems.

In 1-D transient solvers, the approach to describe unsteady friction is to decompose friction in two components: a steady-state friction component calculated by classic pipe resistance formulas based on average velocity (*e.g.*, Colebrook-White's or Hagen-Poiseiulle's formula for turbulent or laminar flow, respectively); and an unsteady friction component described based on average velocity, local acceleration or past time history of velocities. These terms are included in the momentum equation that is solved with the mass balance equation, typically, by the Method of Characteristics. Several boundary and internal conditions can be easily implemented.

Alternatively, two-dimensional (2-D) models can be used to describe these flows. Although more precise, the main disadvantages of 2-D models are the difficulties in the definition of boundary conditions, and the high computational time and memory storage.

One of the most well-know two-dimensional model was presented by Vardy and Hwang (Vardy and Hwang 1991), and was implemented herein with some modifications. The model is based on a discretization of the section of the pipe in several hollow cylinders along the whole length of the pipe. The analysis regards which single shell, calculating the local axial velocity component and the lateral mass flux between cylinders. The pressure is assumed uniform at any cross-section considering that axial variations are much greater than radial variation in normal transient pipe flow problems, this is the reason why it is not a pure 2-D model and is usually referred as a quasi-2-D model.

3.2 Cylinder model

3.2.1 *Momentum and mass-balance equations in 1-D models*

The basic one-dimensional differential equations for transient flows in pressurized pipes are the momentum and the mass-balance equations (Chaudhry 1987; Wylie and Streeter 1993; Almeida and Koelle 1992):

$$g\frac{\partial H}{\partial x} + V\frac{\partial V}{\partial x} + \frac{\partial V}{\partial t} + f\frac{V|V|}{2D} = 0 \tag{1}$$

$$V\frac{\partial H}{\partial x} + \frac{\partial H}{\partial t} + \frac{c^2}{g}\frac{\partial V}{\partial x} = 0 \tag{2}$$

2-D models are extension of the standard 1-D water hammer equations. The pipe is divided in concentric cylinders and additional terms are included in the mass balance and momentum equations to take into account mass fluxes between cylinders and shear stress as a function of the velocity profile. These models calculate both pressure and velocity profiles in each cross section.

3.2.2 Continuity Equation

The continuity equation in 2-D models must incorporate the axial velocity u_j and the laterals velocities between adjacent cylinders (Figure 5).
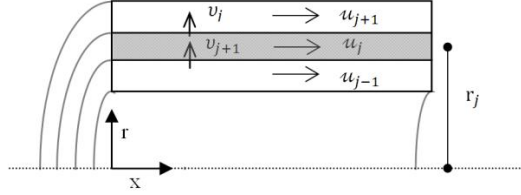

Figure 5 – Discretization of flow into a finite number of cylinders

For each cylinder that extend along the whole length of the pipe can be written the continuity equation as follows (Vardy and Hwang 1991):

$$-\frac{\partial}{\partial x}\left(2\pi\rho r_j \Delta r_j\right)\delta x + 2\pi\rho\left(r_j - \frac{1}{2}\Delta r_j\right)v_{j-1}\delta x - 2\pi\rho\left(r_j + \frac{1}{2}\Delta r_j\right)v_{j-1}\delta x = \frac{\partial}{\partial t}\left(2\pi\rho r_j \Delta r_j\right)\delta x \quad (3)$$

This equation can be written as a function of lateral mass flux per unit length, $\dot{m}_j = 2\pi r\,\rho\,v_j$, being very similar to the continuity equation in 1-D analysis (Eq. 2).

$$u_j\frac{\partial H}{\partial x} + \frac{\partial H}{\partial t} + \frac{c^2}{g}\frac{\partial u_j}{\partial x} = \frac{c^2}{g}\frac{1}{\rho a_j}\left(\dot{m}_{j-1} - \dot{m}_j\right) \quad (4)$$

3.2.3 Momentum Equation

Similarly, momentum equation can be rewritten changing the control volume from the entire pipe section to a small volume element - the concentric cylinder - and regarding the velocity profile defined.

Figure 6 shows the external forces considered in the quasi-two-dimensional model for cylinder j: the friction in the cylinder walls represented by the wall shear stress, τ_{j+1} and τ_j, multiplied by the lateral cylinder area; and the total normal pressure in pipe cross sections described by the product between area A_j and the pressure gradient Δp over the considered volume element.
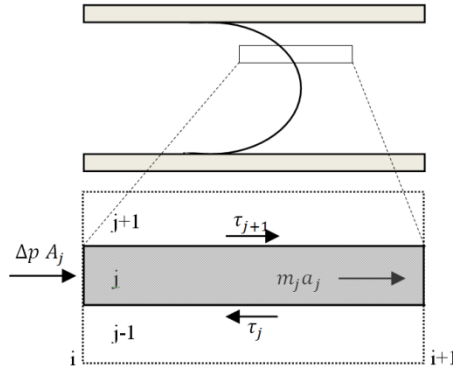

Figure 6 – Forces considered in the momentum equation in 2-D model

Summing all the volumes in the radial direction, it yields the following result:

$$-\sum_{j=1}^{N} \Delta A_j \Delta p + \sum_{j=1}^{N} \left(P_j \tau_j - P_{j+1} \tau_{j+1} \right) = \sum_{j=1}^{N} \Delta m_j a_j \tag{5}$$

Taking into consideration that the pressure gradient Δp is constant for all cylinders between cross sections i and i+1, letting the element size tend to zero and considering that a is the mean acceleration over the pipe radius, the momentum equation can be written as follows:

$$g\frac{\partial H}{\partial x} + \frac{\partial u_j}{\partial t} = \frac{1}{r\rho}\frac{\partial \tau}{\partial r} \tag{6}$$

3.3 Numerical solution

Equations (4) and (6) can be combined to form a pair of Characteristic Equations, valid only in the "characteristic" directions. According to Vardy and Hwang (1991), these equations include the mass lateral flux ($\dot{m} = 2\pi r\rho v$) and the local shear force ($F = 2\pi r\tau$) both per unit length, as follows:

$$\begin{cases} \pm\dfrac{g}{c}\dfrac{dH}{dt} + \dfrac{du_j}{dt} = \dfrac{1}{\rho\,a_j}\left[\dot{m}_{j-1}\left(\dfrac{1}{2}\left(u_{j-1} - u_j\right) \pm c\right) - \dot{m}_j\left(\dfrac{1}{2}\left(u_j - u_{j+1}\right) \pm c\right) + \left(F_{j-1} - F_j\right)\right] \\[2mm] \dfrac{dx}{dt} = u_j \pm c \end{cases} \tag{7-8}$$

At any point along the pipeline, two equations can be written for each cylinder providing a relation between unknowns H, u_j and $\dot{m}_{j-1}$. It should be highlighted that the number of momentum equations must be equal to the number cylinders (J) considered in the radial direction.

The grid system is presented in Figure 7 with spatial division of Δx and the time step is calculated by $\Delta t = \Delta x/c$. The pipe is divided into J cylinders with varying wall thickness. The terms of the left hand side of Equation 7 can be integrated and the terms in the left side can be approximated by finite differences. The term concerning the local shear force must be treated separately for laminar or turbulent flow.
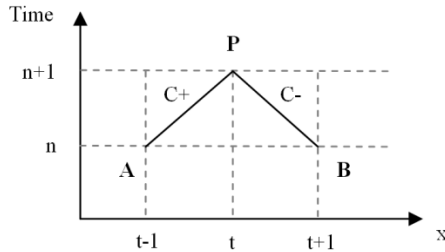

Figure 7 – Grid system for numerical solution

In what concerns the lateral mass flux, its variation along de characteristic line is relatively small for low velocities, and the following approximation was considered (Vardy and Hwang 1991):

$$\int_L^A \dot{m}(u \pm c)\, dt \cong c_0 \dot{m}_A\, \Delta t \tag{9}$$

Using the grid presented in Figure 7, integrating the characteristics equations along the positive and negative characteristics lines and using the approximation in Equation 9, the characteristic equations can be described by the following finite-difference schemes:

$$\frac{g}{c}H_P + u_{P,j} + \theta\left[u_{P,j+1}(-B_j) + u_{P,j}(+A_j + B_j) + u_{P,j-1}(-A_j)\right] +$$
$$\theta\frac{\Delta x}{a_j\rho}(+\dot{m}_{P,j} - \dot{m}_{P,j-1}) \quad = +\frac{g}{c}H_A + u_{A,j} + (1-\theta)\left[u_{A,j-1}(+A_j) + \right. \tag{10}$$
$$\left. u_{A,j}(-A_j - B_j) + u_{A,j+1}(+B_j)\right] + (1-\theta)\frac{\Delta x}{a_j\rho}(-\dot{m}_{A,j} + \dot{m}_{A,j-1})$$

$$+\frac{g}{c}H_P - u_{P,j} + \theta\left[u_{P,j+1}(+B_j) + u_{P,j}(-A_j - B_j) + u_{P,j-1}(+A_j)\right] +$$
$$\theta\frac{\Delta x}{a_j\rho}(+\dot{m}_{P,j} - \dot{m}_{P,j-1}) \quad = +\frac{g}{c}H_B - u_{B,j} + (1-\theta)\left[u_{B,j-1}(-A_j) + \right. \tag{11}$$
$$\left. u_{B,j}(+A_j + B_j) + u_{B,j+1}(-B_j)\right] + (1-\theta)\frac{\Delta x}{a_j\rho}(-\dot{m}_{B,j} + \dot{m}_{B,j-1})$$

Where the coefficients A_j and B_j are as follows:

$$A_j = \frac{1}{r_j - r_{j-1}} \times \frac{2\pi r_j \Delta t\, \nu}{a_j} \text{ and } B_j = \frac{1}{r_{j+1} - r_j} \times \frac{2\pi r_j \Delta t\, \nu}{a_j} \tag{12-13}$$

3.4   Boundary and initial conditions

There were two boundary conditions considered herein: (1) the closure of the downstream end valve and (2) the upstream reservoir.

The valve closure can be described an instantaneous manoeuvre (i.e., duration equal to a time step), for which all the axial velocity components at the valve section are considered zero and the lateral mass fluxes between cylinders are calculated based on Equations (10-11) (Vardy and Hwang 1991). Alternatively, the valve closure can be described by a non-instantaneous manoeuvre, having a certain duration t_F; for this case, the boundary condition is solved as in 1-D models calculating head and average velocity at the valve based on orifice equations and, afterwards, the velocity profile is computed with the same shape as in the previous time step, but with an average value corresponding to the computed average velocity; lateral mass fluxes at the valve are set to zero.

The constant level reservoir at the upstream end is described by setting the mass lateral flux equal to zero and calculating the local velocity for which cylinder based on Equations (10-11) (Vardy and Hwang 1991).

In terms of initial conditions, an uniform velocity profile is considered along the pipeline and model is run for several time steps until a steady velocity profile is reached. The number of time steps taken to reach the initial conditions for laminar flows (resulting in the Hagen-Poiseuille velocity profile) is much higher than for turbulent flows.

3.5 Shear stress

For laminar steady-state flows, there is an analytical formulation that relates velocity and shear stress and that can be used for the definition of the initial data and the implementation of the model during the transient pipe flow:

$$\tau_j = \mu \, \frac{\partial u}{\partial r} \approx \mu \, \frac{u_j - u_{j-1}}{r_j - r_{j-1}} \tag{14}$$

However, for turbulent flows, a reliable turbulence model is needed as there is no analytical solution.

The basic concept of the turbulence models is that components defined as Reynolds stresses $(-\rho \overline{u'_Z u'_R})$ are described according to the Boussinesq hypothesis, which relates the stresses to the eddy viscosity distribution as follows:

$$-\rho \overline{u'_Z u'_R} = \rho \epsilon \, \frac{\partial u_Z}{\partial r} \tag{15}$$

The eddy viscosity is then calculated by a turbulence model. Different models exist (Wilcox, 1993), namely: Piecewise Linear Distribution, Modified Van-Driest Mixing Length Model and Five – Layer Viscosity Distribution.

The total kinematic viscosity is the sum of the laminar kinetic viscosity ν and the eddy viscosity ϵ: $\nu_T = \nu + \epsilon$.

In this research, it was implemented the five layer's model (Wilcox, 1993; Rufelt, 2010) equations are presented in Table 1.

**Table 1 – Five layer's turbulence model implemented**

Region	Total kinematic viscosity	Region
Viscous layer	$\nu_t = \nu$	$0 \leq y_* \leq \dfrac{1}{C_a}$
Buffer I layer	$\nu_t = \nu \, C_a$	$\dfrac{1}{C_a} \leq y_* \leq \dfrac{C_a}{C_B}$
Buffer II layer	$\nu_t = \nu \, C_B \, y_*^2$	$\dfrac{C_a}{C_B} \leq y_* \leq \dfrac{\mathcal{K}}{C_B + \mathcal{K}^2/4C_m R_*}$
Logarithmic region	$\nu_t = \nu \, \mathcal{K} y_* \left(1 - \dfrac{\mathcal{K} y_*}{4 C_m R_*} \right)$	$\dfrac{\mathcal{K}}{C_B + \mathcal{K}^2/4C_m R_*} \leq y_* \leq \dfrac{2 C_m}{\mathcal{K}} \left(1 + \sqrt{1 - C_C/C_m} \right)$
Core region	$\nu_t = \nu \, C_C \, R_*$	$\dfrac{2 C_m}{\mathcal{K}} \left(1 + \sqrt{1 - C_C/C_m} \right) R_* \leq y_* \leq R_*$

4   NUMERICAL RESULTS

The aim of the numerical analysis carried out is a better understanding of the energy dissipation differences between the two models – 1-D and 2-D – and the comparison of 2-D numerical results with the collected data. For this purpose, the pipe system used for carrying out the analysis was the experimental pipeline. Three different situations are presented: numerical analysis of laminar flow conditions, numerical analysis turbulent flow conditions and comparison of numerical results with experimental data for turbulent conditions.

4.1   Numerical analysis of laminar flow conditions

Results obtain by the classic 1-D model (neglecting unsteady friction) and by the Vardy and Brown's cylindrical model for laminar conditions, corresponding to an initial flow of 0.3 L/s (i.e., average velocity equal to 0.01 m/s and *Re*=2000), are presented in Figure 8.
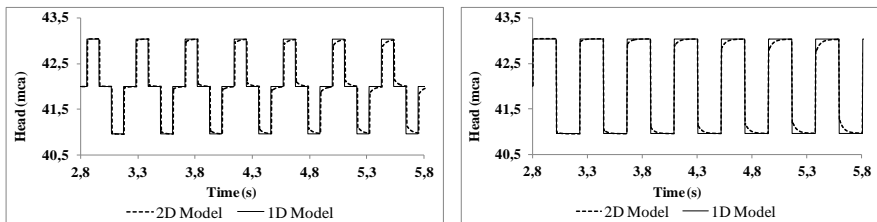
a) at mid-length of the pipeline

b) the downstream end of the pipeline

Figure 8 – Comparison of numerical results obtained by 1-D and 2-D models for laminar flow conditions and for the instantaneous closure of the downstream end valve

The analysis of this figure shows that the pressure variation obtained by the 1-D model at the downstream of the pipe system, after one cycle of the pressure wave propagation, is approximately 0.36% of the initial pressure amplitude. On the other hand, for the same period, the 2D-model leads to a 4.8% reduction of pressure amplitude.

Figure 9 depicts the velocity profiles obtained by the 2-D model at mid-length of the pipeline. The figure shows that:
- At the time when the valve closes (t=ti) the velocity profile is the corresponding to Hagen-Poiseiulle distribution for laminar flow (Figure 9a).
- At t = t_i +0.5L/c, the initial laminar flow profile remains almost unchanged in the core region and shows a pronounced flow reversal close to the wall (Figure 9b). This behaviour is consistent with the fact that the average velocity is zero. This flow reversal close to the pipe-wall is responsible for a large wall shear stress that cannot be accurately predicted by a quasi-steady state friction in 1-D models because, in this period, the average velocity is zero.
- After the reflection of the wave in the reservoir, the velocity profile starts assuming a uniform negative velocity (Figure 9c) and the increase of velocity happens near the pipe wall.
- One quarter of a period later, after the reflection of the wave in the valve, the average velocity is zero (Figure 9d).
- Finally, one period after the closing of the valve, the velocity profile presents a distribution corresponding to the initial conditions but the average velocity decreases, when compared with the initial conditions, due to the energy dissipation (Figure 9e).
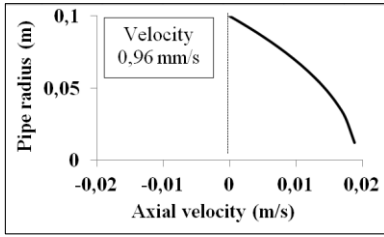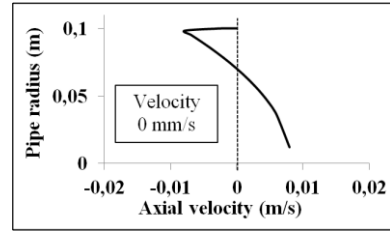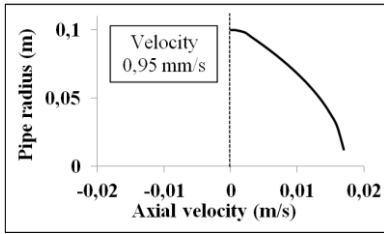
a) Immediately after closing the valve ($t=t_i$)
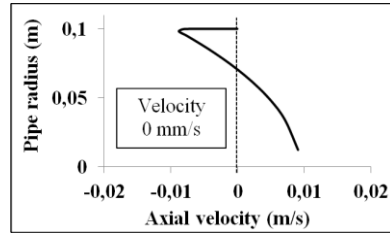
b) One quarter of period after closing the valve ($t=t_i+0.5L/c$)
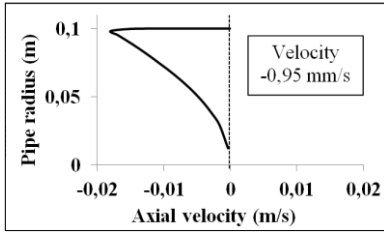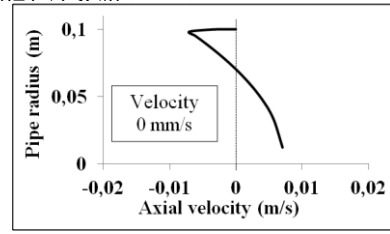

c) Half of period after closing the valve ($t= t_i +L/c$)

d) Three quarters of period after closing the valve ($t= t_i +1.5L/c$)

e) One period after closing the valve ($t= t_i +2L/c$)

f) One and a quarter of period after closing the valve ($t= t_i +2.5L/c$)

Figure 9 – Radial distribution of axial velocity at mid-length of pipe in laminar flow

4.2 Numerical analysis of turbulent flow conditions

The analysis of turbulent conditions is carried out for three different initial flow rates – Q=10.8 L/s (U= 0.57.m/s), Q=5.5 L/s (U = 0.17 m/s) and Q= 2 L/s (U=0.06 m/s) – and for two valve closure times, $t_F = \Delta t$ (instantaneous manoeuvre) and $t_F = 0.2$ s. Results are presented in Figures 10 to 12.
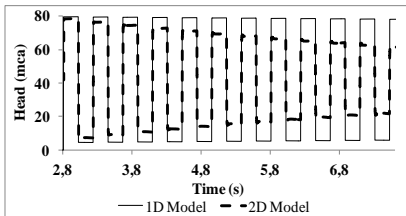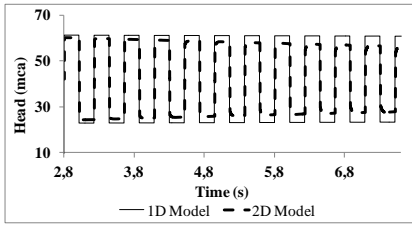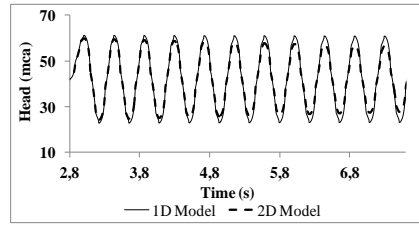

a) Instantaneous closing of the valve
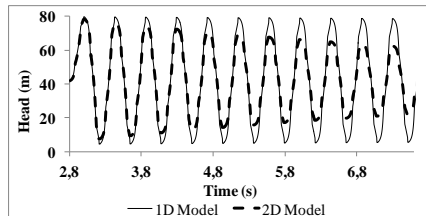
b) Linear valve manuervre (t=0.2s)

Figure 10 – Numerical results obtained by 1-D and 2-D models for turbulent flow Q=10.8 l/s
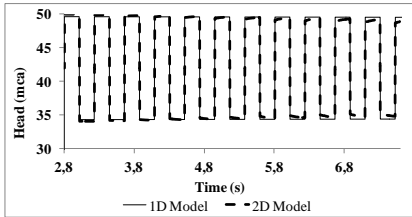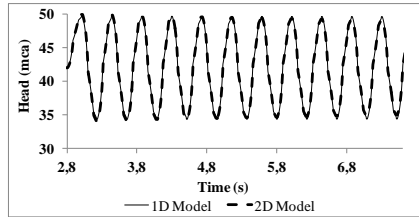
a) Instantaneous closing of the valve   b) Linear valve manuervre (t=0.2s)

Figure 11– Numerical results obtained by 1-D and 2-D models for the turbulent flow Q=5.5 l/s

a) Instantaneous closing of the valve   b) Linear valve manuervre (t=0.2s)

Figure 12 – Numerical results obtained by 1-D and 2-D models for the turbulent flow Q=2 l/s

The pressure wave dissipation between the first and the second pressure peak at the upstream section of the pipeline is present in Table 2. The energy dissipation considerably increases from the 1-D to the 2-D model.

Table 2 – Energy dissipation considering the classic method (1D Model) and the Vardy´s numerical methodology (2D Model)

Flow (l/s)	Amplitude reduction of the pressure wave (one cycle)	
	1D – Model	2D – Model
10.8	0.31 %	5.47 %
5.5	0.18 %	2.58 %
2.2	0.08 %	1.40 %

The turbulent velocity profile obtained is depicted in Figure 13. This profile presents a considerably different shape from the one obtained for laminar flow in steady-state conditions (Figures 9a and 13a). However, the behaviour of the velocity profile during the transient regime is equivalent to the laminar flow described previously as it invers near de wall and maintains its shape in the core region (Figures 9b and 13b)..
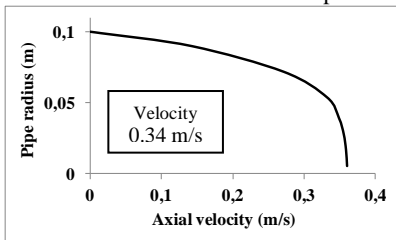
Velocity 0.34 m/s

Velocity 0 m/s
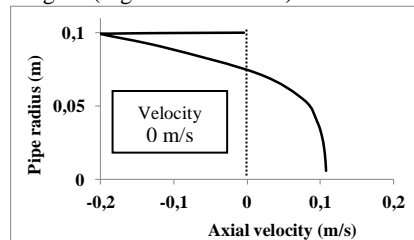
a) Immediately after closing the valve ($t=t_i$) b) One quarter of period after closing the valve ($t=t_i+0.5L/c$)

Figure 13 – Radial distribution of axial velocity at mid-length of pipe in turbulent flow

4.3 Numerical versus experimental results

Despite the referred difficulties faced in the experimental data collection and the corresponding uncertainties of experimental data, numerical results obtained by 1-D and 2-D models are compared with collected data in March 2012 (Day 3) and in May 2012 (after installing the electric filter), as depicted in Figure 13. This figure shows that (i) the maximum pressure is reasonably well described by both models; (ii) however, none of the numerical models describes minimum pressures and pressure wave phase and shape, propagating the numerical pressure wave much faster than the observed pressure wave. The main reason for this is the presence of air in small pockets along the pipeline, behaving like small springs that delay the pressure wave propagation.
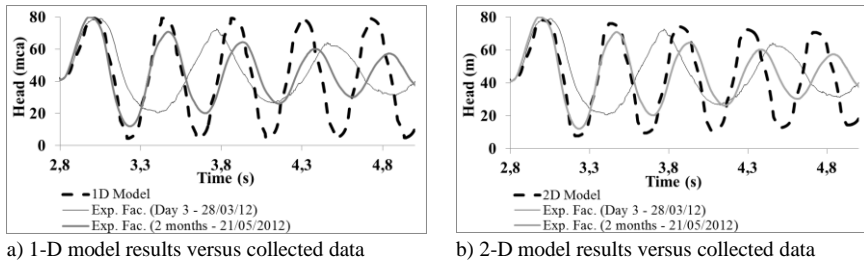
a) 1-D model results versus collected data   b) 2-D model results versus collected data

Figure 14– Comparison between numerical results and collected data for Q=10.8 l/s.

5 CONCLUSIONS AND FUTURE WORK

This paper presented the first experimental results obtained in a new experimental facility. The main difficulties faced in data collection were reported: the electric noise in the pressure signal induced by the pump frequency converter and the presence of small air pockets along the pipeline. Short-term measures will be taken to overcome these problems, namely the installation of air valves along the pipeline and the installation of electric filters in the frequency converter. In order to collect pipe wall deformation, wall shear stress and velocity fields during transient events, additional instrumentation will be installed: strain gauges, hot-films and a transparent box with PIV measurements.

The paper shows as well the comparison of classic 1-D and quasi 2-D models. Results have shown that the latter leads to a much higher energy dissipation in the transient pressure variation than the former. The next steps in the numerical analysis are: (i) the comparison of different turbulent flow models; (i) the analysis of the effect of gradually dampened eddy viscosity distribution; (iii) the comparison of quasi 2-D models with 1-D models with different unsteady friction models (iv) the comparison of the velocity profiles using the PIV equipment with the results obtained for different turbulent flow models; (v) the analysis of the real energy dissipation and the comparison with the model results.

6 ACKNOWLEDGMENTS

7   REFERENCES

Almeida, A. B., and Koelle, E. (1992). Fluid Transients in Pipe Networks., Computational Mechanics Publications, Elsevier Applied Science, Southampton, UK.

Ariyaratne, C., Shuisheng He, and Vardy, A. E.(2010). "Wall friction and turbulence dynamics in decelerating pipe flows." 810-821.

Brunone, B., Golia, U. M., and Greco, M. (1995). "Effects of Two-Dimensionality on Pipe Transients Modelling." Journal of Hydraulic Engineering, ASCE, 121(12), 906-912.

Chaudhry, M. H. (1987). Applied Hydraulic Transients, 2nd Edition Ed., Litton Educational Publishing Inc., Van Nostrand Reinhold Co, New York, USA.

Eichinger, P., and Lein, G. (1992). "The influence of friction on unsteady pipe flow." Bettess & Watts, Balkema, Rotterdam, 41-50.

Hino, M., Sawamoto, M., and Takasu, S. (1977). "Study on the Transition to Turbulence and Frictional Coefficient in an Oscillatory Pipe Flow." Transactions of JSCE, 9, 282-285.

Pezzinga, G. (1999). "Quasi-2D Model for unsteady Flow in Pipe Networks." Journal of Hydraulic Engineering, ASCE, 125(7), 676-685.

Ramos, H., Borga, A., Covas, D., and Loureiro, D. (2004). "Surge damping analysis in pipe systems: modelling and experiments." Journal of Hydraulic Research, 42(4), 413-425.

Rufelt, A. (2010). "Numerical Studies of Unsteadt Friction in Transient Pipe Flow" Master of Science Thesis, KTH Computer Science and Communication, Sweden.

Shuy, E. B. (1996). "Wall shear stress in accelerating and desacelerating turbulent pipe flows." Journal of Hydraulic Research, 34(2).

Silva-Araya, W. F., and Chaudhry, M. H. (1997). "Computation of energy dissipation in transient flow." Journal of Hydraulic Engineering, ASCE, 123(2), 108-115.

Trikha, A. K. (1975). "An efficient method for simulating frequency-dependent friction in transient liquid flow." Journal of Fluids Engineering, Trans. ASME, 97(1), 97-105.

Vardy, A. E., and Hwang, K. L. (1991). "A characteristic model of transient friction in pipes." Journal of Hydraulic Research, 29(5), 669-684.

Vardy, A. E., Hwang, K. L., and Brown, J. (1993). "A weighting function model of transient turbulent pipe friction." Journal of Hydraulic Research, 31(4), 533-548.

Vitkovsky, J. P., Lambert, M. F., and Simpson, A. R. (2000). "Advances in unsteady friction modelling in transient pipe flow." BHR Group Ltd., Publication No. 39, Suffolk, UK, 471-498.

Wilcox, D.C. (1993)"Turbulence Modelling for CFD".1st Edition. DCW Industries, Inc. United States of America by Griffin Printing, Glendale, California. ISBN 0-9636051-0-0

Wylie, E. B., and Streeter, V. L. (1993). Fluid Transients in Systems., Prentice Hall, Englewood Cliffs, N.J..

Zielke, W. (1968). "Frequency-dependent friction in transient pipe flow." Journal of Basic Engineering, Trans. ASME, Series D, 90(1), 109-115.